

Investigation of Carbon Composition for Electrochemical Properties as PEMFC Cathode Catalyst

Vuri Ayu Setyowati^{1,a*}, Diah Susanti^{2,b}, Lukman Noerochim^{2,c},
Eriek Wahyu Restu Widodo^{1,d} and Mohammad Yusuf Sulaiman^{1,e}

¹Adhi Tama Surabaya Institute of Technology, Indonesia

²Sepuluh Nopember Institute of Technology, Indonesia

^avuri@itats.ac.id, ^bsantiche@mat-eng.its.ac.id, ^clukman@mat-eng.its.ac.id, ^deriek@itats.ac.id,
^emoh.yusufsulaiman@gmail.com

Keywords: Fe-N-C catalyst, fuel cell, PEMFC

Abstract. Nitrogen –doped carbon material using non-precious metal was developed as catalyst fuel cell (PEMFC). In the PEMFC, the cathode reaction occurs three times slower than anode reaction. Oxygen reduction reaction (ORR) in the cathode has major limit performance. Pt/C was used as high-cost catalyst materials, but many researchers are concerned to improve cathode catalyst performance using high-performance and low-cost materials. Nitrogen based active sites on carbon has important role for oxygen reduction reactions process. In this study, compositions of carbon for Fe-N-C were investigated to understand the electrochemical properties and morphological analysis. Urea and PVP as nitrogen (N) source were mixed with graphite (Gt). The ratio of Gt and N were 1:1, 3:1, and 1:3. The mixture was added to FeCl₃.6H₂O dissolved in ethanol to produce Fe-N/C catalyst. Subsequently, powder was induced to the furnace for pyrolysis. The catalyst products were analyzed using Potentiostat to show the electrochemical properties of catalyst, while X-Ray Diffractometer (XRD) was used to know the compound or phases after catalyst syntheses. Moreover, Scanning Electron Microscope – Energy Dispersive X-Ray (SEM-EDX) was used to identify the morphology and the chemical compositions of catalyst. As a result, Fe – Gt : N = 1:3 catalyst had the greatest electrochemical properties which is identified by the large area of CV curve. This catalyst also had the highest current density for reduction reaction. The presence of Fe₂O₃ and FeS caused the degreasing of catalytic activity. This research concluded that carbon composition had an important rule to improve the ORR activity.

Introduction

Today, human life is very dependent on electrical energy. Almost all human needs including transportation, communication and others, need electricity. Electricity is obtained from various power plants, such as coal, oil, gas, nuclear and renewable sources [1]. The increasing needs for electricity makes electricity consumption higher, thus making the mindset about electricity generation changed. Currently, many are included in the characteristics of power generation, in which environmentally friendly and renewable quality are some of them. Green technology can be applied to decrease the global warming effect. Fuel cell, solar cell, and energy-conversion materials are part of green technology to generate less energy consumption and less pollution. Fuel cell provides clean and efficient mechanism for energy conversion. There are many types of fuel cell but PEMFC has the largest application range. Many research have studied PEMFC [2]. The use of PEMFC has many advantages, such as high energy density, high power density, high energy conversion efficiency, low operating temperature, and environmentally friendly trait. However, the manufacturing of PEMFC in industrial and commercial scale are hampered because it requires high costs. The catalyst is made from platinum-based materials and the PEMFC's stability is not high enough [3]. The cost of platinum-based catalyst is about 40% of the total fuel cell cost [4]. To overcome the high cost of such platinum-based catalysts, there are two approaches: 1) Reducing the amount of Pt in the catalyst, and 2) Replacing Pt with other materials [4-6]. Platinum is the catalyst for Oxygen Reduction Reaction (ORR) which is an important reaction in the fuel cell. Thus, platinum is substituted with low cost

material that still has the needed ORR [7]. One type of catalyst in PEMFC which is not based on Pt is a metal-nitrogen-based catalyst type of carbon, in which metals that can be used include Fe, Ni, Co and Mn [4]. The Fe, Ni, Co and Mn are 3d-transition metals which can enhance the intrinsic activity by 2-4 times due to a change in morphology, electronic properties, inhibition towards anion adsorption and surface sensitive factors [8]. The nitrogen role in M-N-C is to increase the onset potentials and current densities for ORR [9]. Nitrogen was used as the most important dopant to generate active sites, because nitrogen atom has five electron valences for bonding and has similar atomic size to carbon. It is called as nitrogen-doped carbon [10]. Pyridinic has significant role for oxygen reduction and the catalytic performance is proportional with this nitrogen functional group. In addition, metal and nitrogen interaction is essential for the generation of an active site [11]. On the other hand, carbon is used because carbon has high conductivity, high mechanical and chemical stability and easy modification. In addition, carbon can increase the catalytical activity [12]. Iron as metal precursor also affected catalytic activity because of the Fe-N-C structure. Iron has oxidation state of Fe^{3+} which is formed by Fe-N4 structure, and has important role to adsorb O_2 . This process enhances ORR activity [13]. However, the role of carbon used in the catalyst still needs further research. Therefore, this research aims to study the carbon composition in cathode catalyst PEMFC.

Materials and Method

The Fe-N/C catalysts were prepared by mixing main materials. Catalysts were synthesized using $FeCl_3 \cdot 6H_2O$ as metal precursor, graphite as carbon doping, and urea as nitrogen source. The required amount of $FeCl_3 \cdot 6H_2O$ was added in different ratio of carbon and nitrogen. PVP was also used as precursor for nitrogen-doped carbon catalyst. There are several compositions utilized to observe the effect of carbon content and nitrogen ratio (Gt:N) which are 1:1, 1:3, and 3:1 in the catalyst. Briefly, PVP and urea Fe were dissolved in 50 mL of aquades. The mixture was stirred for 15 minutes. Then carbon was added and stirred for 12 hours at room temperature. The obtained mixture was dried at $70^\circ C$ to remove water content and to produce C-N catalyst powder. Fe content was fixed at 7wt% from $FeCl_3 \cdot 6H_2O$ and mixed with C-N powder using ethanol solvent. The remaining dry mixture was pyrolyzed in vacuum furnace under N_2 atmosphere at $700^\circ C$. The powder of Fe-N/C catalysts was then obtained. Furthermore, electrochemical and physical properties were characterized. CV was measured using potentiostat using potential range of $-0.15 V - 0.85 V$. Physical characterizations consist of Scanning Electron Microscope (SEM) to identify the morphology, Energy Dispersive X-Ray EDX to identify the chemical composition, and X-ray diffraction (XRD) to determine compound or phases.

Results and Discussions

The Cycle Voltammograms (CV) curve is shown by Fig.1. CV curves provides information on the electrochemical oxygen reduction properties of the catalysts which was performed in 0.1 M $HClO_4$ solution. Every catalyst has a reduction peak and an oxidation peak. The oxidation peak around 923 mV to 950mV determines quasi "reversible" reaction and confirms the diffusion-controlled process [14]. The reduction peak happened at 818 mV to 823Mv, while the second reduction peaks appeared at 400mV to 419mV. Each of catalyst composition has different peak position of oxidation and reduction, and also has different current density. 1:3 of $Fe^{2+} : Fe^{3+}$ catalyst reduction peak shifted negatively, and its oxidation peak shifted positively. If cathodic peak potential is higher, it means that its valence can change active sites at the catalyst, and the electron transfer between active metal center and electrode is faster [15] The presence of reduction and oxidation peaks of catalyst indicates that there is no reduction and oxidation reaction, and that free ligands cannot be attributed on metal centers [14,16]. Despite that, the voltammograms shapes show potential capacitive response. It has linear correlation with surface area. High current of capacity has high surface area and contributes to create the surface functional groups [17]. Increasing nitrogen content affects the large share of CV curve and has the highest current density. Fe- Gt: N = 3:1 catalyst has the highest carbon proportion and it has the lowest current density. The figure also shows the smallest area of capacitive response. Nitrogen

contributes to the production of nitrogen functional groups after pyrolysis. Fe- Gt: N = 1:3 catalyst has oxygen reduction peak at 0.341V which is higher than Fe- Gt: N = 3:1 at 0,364 V, indicating high oxygen reduction reaction that was increased by high nitrogen functional groups [18].

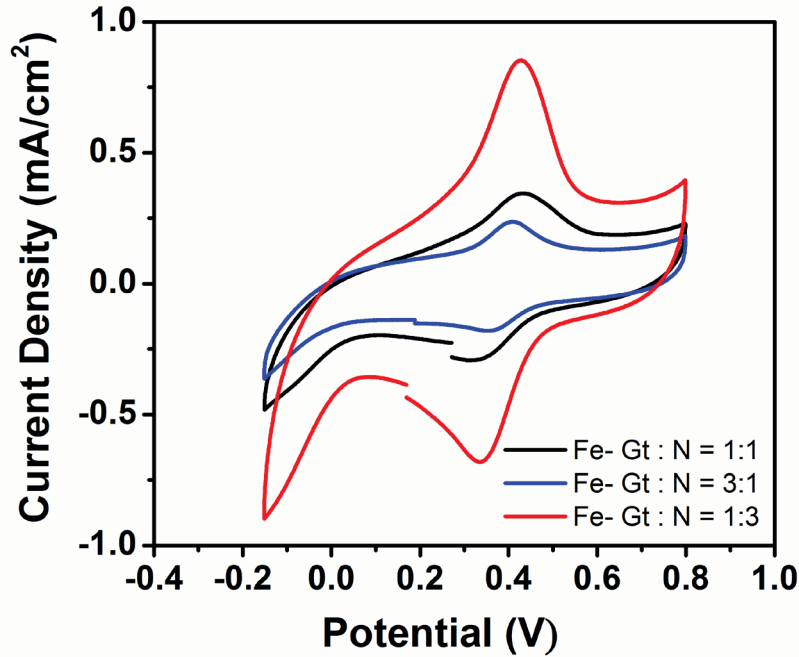


Fig.1. Cyclic voltammograms of various carbon and nitrogen ratio of Fe- Gt: N catalyst in 0.1 M HClO_4 solution at a scan rate of 10 mV s^{-1}

The morphology of the obtained catalyst powder is observed by SEM as shown in Fig.2. Particle distribution before pyrolysis (Fig. 2 a and b) has more agglomerates than after pyrolysis (Fig. 2 c and d). There are many agglomeration of particles occurring in the untreated catalyst, while equal particle distribution happens in the treated catalyst. Pyrolysis as catalyst treatment has an important role to increase catalytic activity. Homogenous particle that has low porosity can be obtained from pyrolyzed catalyst. Dark space of SEM image is identified as porous. Agglomerations contribute to more porosity as displayed by figure b. Low particles agglomeration promotes high nanoparticles dispersion [19].

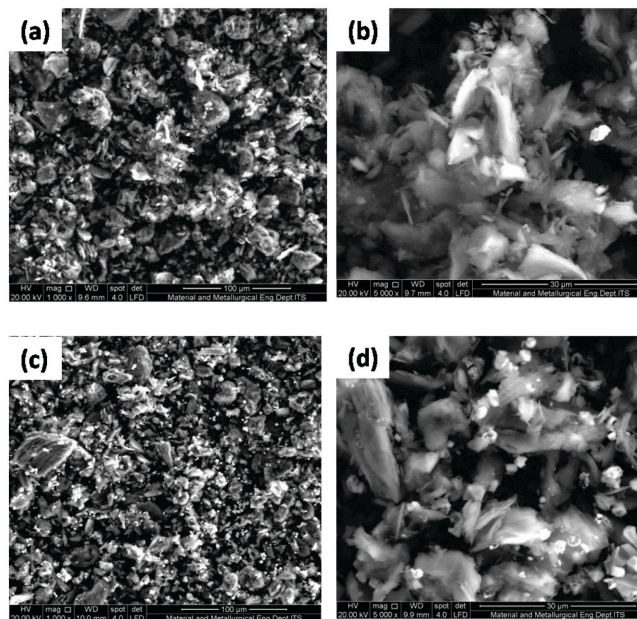


Fig.2. SEM of Fe – Gt : N catalyst using ratio of Gt : N = 3:1 (a) Before pyrolysis 1000x magnification (b) Before pyrolysis 5000x magnification (c) After pyrolysis 1000x magnification (d) After pyrolysis 1000x magnification

Catalyst particle is one of main requirements of good catalyst. The particles ensure that the electrons are supplied to or taken away from the reaction site. Electronic conductivity is usually provided by a carbon support onto which the catalyst particles are supported. It has important role to yield activity in which lower H_2O_2 was produced. The pathway of the ORR is as follow.

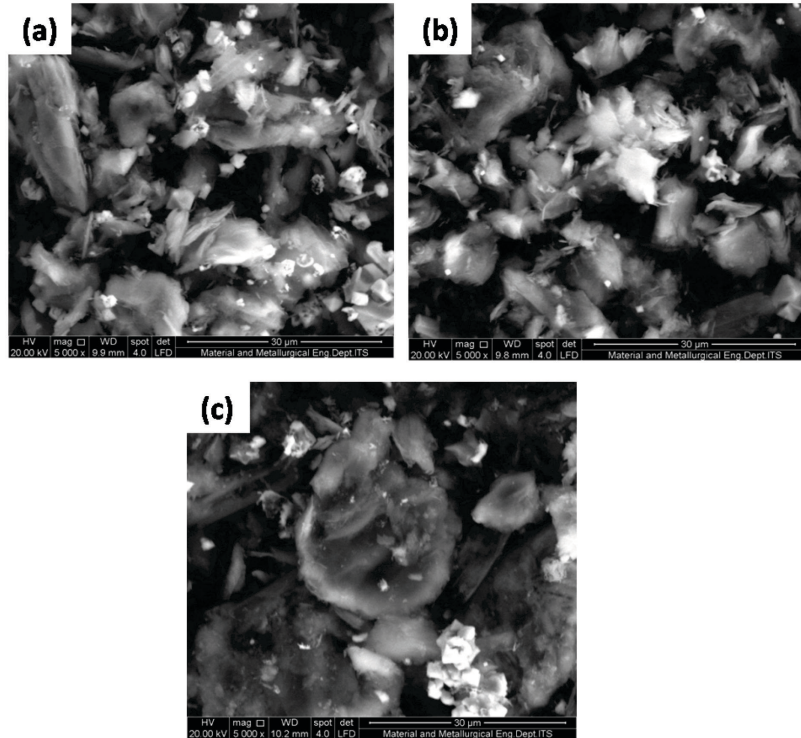


Fig.3. SEM of Fe – Gt : N catalyst using variation ratio of Gt : N (a) Gt : N = 1:1 (b) Gt : N = 3:1 (c) Gt : N = 1:3 in 10.000x magnification

Morphological structures of Fe – Gt : N catalysts are observed as shown in Fig 3. Carbon particles and nitrogen particles can also be identified from Fig 3 where dark and light spots were identified as carbon and nitrogen particles, respectively. SEM image of catalyst using lowest nitrogen content has big particle as shown as the black area of Figure C and it has nitrogen agglomeration. Fe – Gt : N = 1:1 catalyst which is equal in portion of C and N content, has uniformed particle distributions and homogenous particle size of nitrogen. All of pyrolyzed catalysts have dense particles because of iron precursor. Iron cannot be specifically identified by SEM image, but iron interacts with carbon to exhibit surface rearrangement [21].

Fig.4 illustrates that iron compounds were produced after pyrolysis. All of catalyst using various carbon-nitrogen content has no Fe diffraction peak at $2\theta = 45^\circ$. However, catalysts using various graphite and urea content have Carbon (C), FeS, Fe_2O_3 , and Fe_3C peaks. Slight peak which appears at $2\theta = 24.7^\circ$ was identified as graphite peak [4]. The diffraction peak of Fe_2O_3 was located at $35,67^\circ$ and has low intensity belonging to the lowest nitrogen source. The lowest urea content of catalyst presents the highest peak of Fe_2O_3 (JCPDS, PDF# 391346). According to previous research, the Fe_2O_3 nanoparticles play a role as template for the formation of vesicular structure [22]. However, FeS compound was detected from Fe – Gt : N = 1:3 because more urea and PVP were added. The existence of FeS decreased catalytic performance [23]. Peak diffractions at $2\theta = 44.6^\circ$, 54.4° , and 76° contribute to Fe_3C (JCPDS, PDF# 350772). Fe – Gt : N = 3:1 clearly reached peak at $2\theta = 76^\circ$ because of its highest carbon content. The behavior of transition metal catalyst and carbon systems are classified as stoichiometric carbides. Fe_3C is stable under high temperature. This catalyst also has

narrow peaks at $2\theta = 44.6^\circ$ indicating that amorphous carbon has arranged iron compound. Pyrolyzed catalyst has more iron compound peaks compared to when without pyrolysis.

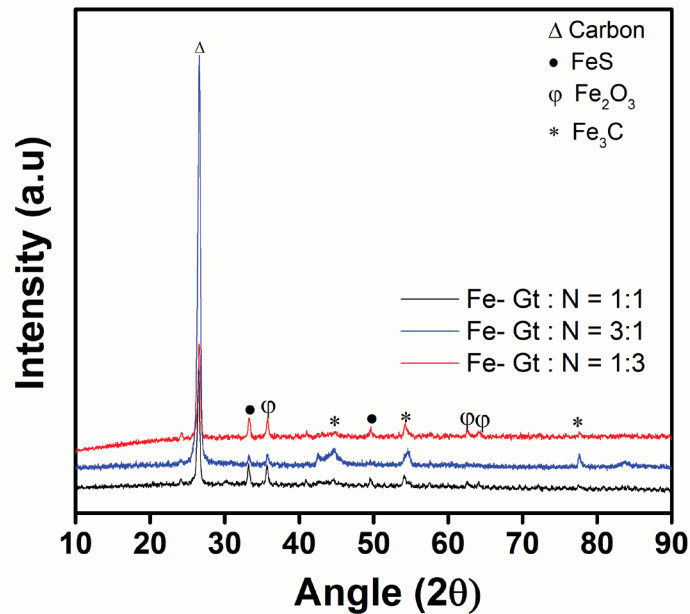


Figure 4. XRD pattern of variation composition for graphite and nitrogen

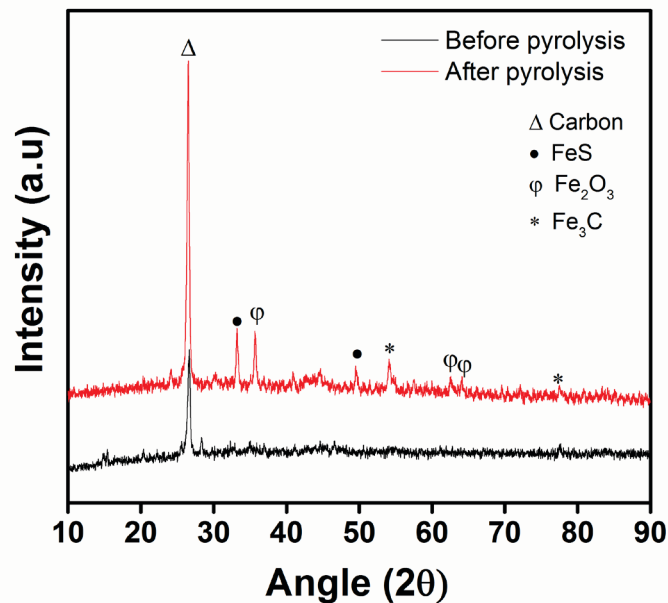


Figure 5. XRD pattern of before and after pyrolyzed catalyst

Fig.5 shows the comparison of diffraction peak for catalyst with and without pyrolysis. Single peak of graphitic carbon diffraction is determined at $2\theta = 24.7^\circ$ and it has lower intensity than pyrolyzed catalyst. The formation of active sites for catalyst is obtained from heat treatment process. Iron content is interacted to nitrogen doped carbon surface and promoted to form the active sites to increase catalytic activity [24]. Catalyst functional groups were formed during initial pyrolysis in which decomposition between ligand and metal ions on carbon support structure happened. Many researchers used acid leaching to remove the residual process, but it was not used in this study. This is because the iron compound influenced the catalytic activity [25].

Summary

Various carbon and nitrogen ratio of catalysts have different electrochemical properties and particles morphology. The highest nitrogen has the most capacitive response using CV analysis.

Fe – Gt : N = 1:3 catalyst has the highest current density. Reduction and oxidation peak of catalysts were located on different potential for various catalysts. Potential of reduction peak is negatively shift and it is opposite with potential oxidation peak. For XRD analysis, Fe – Gt : N = 1:3 catalyst has the lowest Fe₂O₃ peak indicating low amount of oxidized iron. Fe₂O₃ and Fe₃C have important role to improve the electrochemical properties.

Acknowledgements

This work is supported by Ministry of Research Technology and Higher Education of Indonesia (120/SP2H/LT/DRPM/2018) as research funding for collaboration research scheme . The first author would like to thank laboratory of Materials Engineering Department from Institut Teknologi Sepuluh Nopember (ITS).

References

- [1] B. Zohuri, Application of compact heat exchangers for combined cycle driven efficiency in next generation nuclear power plants: a novel approach, Springer, 2015.
- [2] O.Z. Sharaf, M.F. Orhan, Renewable and Sustainable Energy Reviews 32 (2014) 810.
- [3] J. Wang, S. Li, G. Zhu, W. Zhao, R. Chen, M. Pan, Journal of Power Sources 240 (2013) 381.
- [4] A. Serov, M.J. Workman, K. Artyushkova, P. Atanassov, G. McCool, S. McKinney, H. Romero, B. Halevi, T. Stephenson, Journal of Power Sources 327 (2016) 557.
- [5] A. Serov, M. Padilla, A.J. Roy, P. Atanassov, T. Sakamoto, K. Asazawa, H. Tanaka, Angewandte Chemie International Edition 53 (2014) 10336.
- [6] S. Stariha, K. Artyushkova, M.J. Workman, A. Serov, S. Mckinney, B. Halevi, P. Atanassov, Journal of Power Sources 326 (2016) 43.
- [7] H. Deng, Q. Li, J. Liu, F. Wang, Carbon 112 (2017) 219.
- [8] S. Mukerjee, S. Srinivasan, Journal of Electroanalytical Chemistry 357 (1993) 201.
- [9] M. Li, Z. Liu, F. Wang, J. Xuan, Journal of energy chemistry 26 (2017) 422.
- [10] Y. Tang, B.L. Allen, D.R. Kauffman, A. Star, Journal of the American Chemical Society 131 (2009) 13200.
- [11] P. Wang, Z. Ma, Z. Zhao, L. Jia, Journal of Electroanalytical Chemistry 611 (2007) 87.
- [12] B. Huang, L. Peng, F. Yang, Y. Liu, Z. Xie, Journal of energy chemistry 26 (2017) 712.
- [13] V.A. Setyowati, H.-C. Huang, C.-C. Liu, C.-H. Wang, Electrochimica Acta 211 (2016) 933.
- [14] V. Paredes-García, D. Venegas-Yazigi, R.O. Latorre, E. Spodine, Polyhedron 25 (2006) 2026.
- [15] R. Jiang, D. Chu, Journal of Power Sources 245 (2014) 352.
- [16] R. Zheng, Z. Mo, S. Liao, H. Song, Z. Fu, P. Huang, Carbon 69 (2014) 132.
- [17] F. Pérez-Alonso, M.A. Salam, T. Herranz, J.G. de La Fuente, S. Al-Thabaiti, S. Basahel, M. Peña, J. Fierro, S. Rojas, Journal of power sources 240 (2013) 494.
- [18] H. Li, H.-J. Zhang, X. Li, S. Zheng, B. Zhao, J. Yang, International Journal of Hydrogen Energy 39 (2014) 3198.
- [19] X. Ren, B. Liao, Y. Li, P. Zhang, L. Deng, Y. Gao, Electrochimica Acta 228 (2017) 36.
- [20] S.-T. Chang, H.-C. Hsu, H.-C. Huang, C.-H. Wang, H.-Y. Du, L.-C. Chen, J.-F. Lee, K.-H. Chen, International Journal of Hydrogen Energy 37 (2012) 13755.
- [21] J. Zhang, D. He, H. Su, X. Chen, M. Pan, S. Mu, Journal of Materials Chemistry A 2 (2014) 1242.
- [22] Z. Mo, H. Peng, H. Liang, S. Liao, Electrochimica Acta 99 (2013) 30.
- [23] G. Wu, C.M. Johnston, N.H. Mack, K. Artyushkova, M. Ferrandon, M. Nelson, J.S. Lezama-Pacheco, S.D. Conradson, K.L. More, D.J. Myers, P. Zelenay, Journal of Materials Chemistry 21 (2011) 11392.
- [24] M.-Q. Wang, C. Ye, M. Wang, T.-H. Li, Y.-N. Yu, S.-J. Bao, Energy Storage Materials 11 (2018) 112.
- [25] Z. Mo, H. Peng, H. Liang, S. Liao, Electrochimica Acta 99 (2013) 30.